An Optical Sensor for Tracking Hand Articulations

L. Wang, T. Meydan, and P. Williams
Wolfson Centre for Magnetics
School of Engineering, Cardiff University
Cardiff, Wales, UK
Email: Meydan@cardiff.ac.uk

***Abstract*—Recognizing and tracking articulations of the human hand is key to the development of areas such as robotics, virtual reality systems and physical rehabilitation. Based on the principle of crossed-polarization detection, a novel optical sensor with a hinge configuration, is proposed to monitor finger articulation. Using 3D printing technology, we fabricated a lightweight and compact sensor suited to attaching on fingers. The weighted average method was applied to the sensor's output data to determine angular positions corresponding to finger joint articulations. The experimental results show excellent consistency with theoretical predictions. The sensor features good accuracy (±0.5% of full scale) and repeatability, improved sensitivity, and an improved measuring range of 180°. The performance of the sensor is a promising development for monitoring finger articulation. Future work will focus on integrating multiple sensors as part of an instrumented glove to evaluate the true potential for monitoring hand articulation.**

Keywords—optical sensor; polarization; hand motion tracking; 3D printing; sensing techniques; rehabilitation.

I. INTRODUCTION

Since the 1970s, hand motion tracking has gained considerable attention in both academia and industry [1, 2]. Various sensing technologies including resistance flex sensors [3], optical fibre techniques [4], magnetic sensing elements [5], and Inertial Measurement Units (IMU) [6], have been investigated for capturing hand movements. Many of these methods either lack accuracy or require complex and time-consuming calibration procedures. Sensors may also possess a limited angular range and/or suffer from significant drift errors. There is a clear need to address these problems by developing new improved sensing technologies.

We have previously reported the use of a polarization technique for monitoring hand articulation [7]. Although some rotational sensors or encoders using polarization techniques have been presented elsewhere [8, 9], they have focused on military or commercial aircraft applications and not human motion tracking. In our previous work, we presented an optical sensor based on the principle of crossed-polarization detection. The measuring range of 90°, however, is not sufficient to monitor the full range of articulation in metacarpophalangeal (MCP) and proximal interphalangeal (PIP) joints. Secondly, the sensitivity is not constant but varies as a function of angle.

To tackle the above problems, here we describe an improved optical sensor, based on a hinge design, with an expanded measuring range of 180°. The sensor's design, characterization method and performance results will be discussed in the following sections.

This research is jointly sponsored by China Scholarship Council (CSC) and Cardiff University.

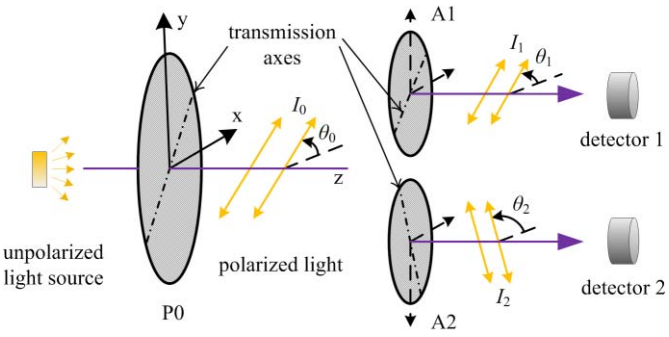

Fig. 1. The schematic diagram of the polarized optical sensor.

II. SENSOR DESIGN

A. Principle of operation

As shown in Fig. 1, the optical sensor consists of a single light source, a linear polarizer P0, two analyzers A1 and A2, and two photodetectors. Passing through P0, the incident light is polarized in the direction of the transmission axis at an angle θ_0 to the x-axis and then split into two separate channels. Each channel has its own analyzer and photodetector providing simultaneous outputs. The two analyzers, A1 and A2, are oriented with their transmission axes at 45° to each other. This ensures that at least one sensor will be operated in the region with maximum sensitivity and linearity. In the following text, we refer to the upper channel in Fig. 1 as 'Channel 1', and the bottom one as 'Channel 2'.

According to Malus' Law, the light intensity I_1 and I_2 should obey the following theoretical relationships:

$$I_1 = I_0 \times \cos^2(\theta_1 - \theta_0) \quad (1)$$

$$I_2 = I_0 \times \cos^2(\theta_2 - \theta_0) \quad (2)$$

where I_0 denotes the initial polarized light intensity, and θ_1 and θ_2 denote the transmission angles, relative to the x-axis, for analyzers A1 and A2 respectively.

B. Fabrication Details

Inspired by the articulated structure of finger joints, we developed an optical sensor with a hinge type configuration. The

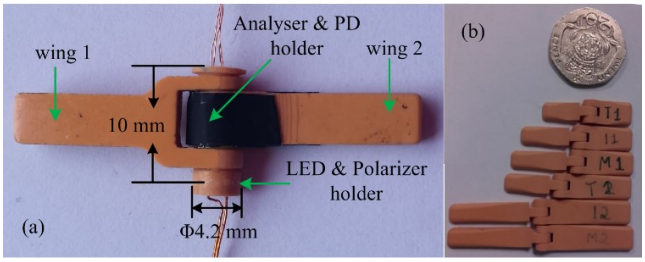

Fig. 3. Image of the complete sensor. (a) The integrated optical sensor. (b) A range of component sizes.

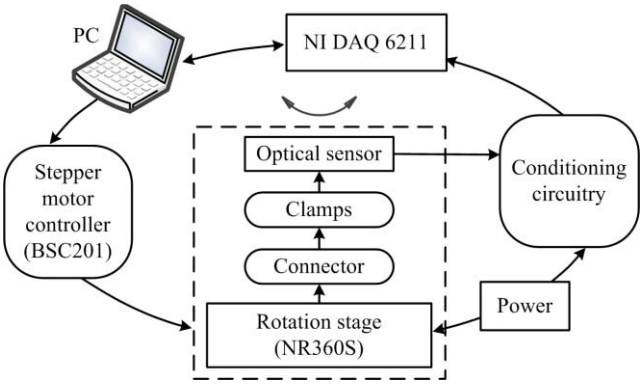

Fig. 2. The block diagram of the automated experimental set-up.

sensor is fabricated using an EnvisionTEC's Perfactory Mini Multi Lens 3D Printer using RCP30 resin. Fig. 3 (a) shows a photograph of the integrated optical sensor with a diameter of 4.2 mm and a width of 10 mm. The sensor is constructed with a range of dimensions, as shown in Fig. 3 (b).

The sensor's polarizer and analyzers are made from commercial linear polarizing film. Two high sensitive PIN photodiodes (TEMD6200FX01) are employed to detect changes in light intensity. The LED source and polarizer P0 are located inside a separate holder and located in wing 1. The two analyzers and photodiodes (PD) are housed inside another holder located inside wing 2. When the wings rotate, the angle between the polarizer and two analyzers also changes, leading to a change in light intensity. The final light intensities are linearly converted to electrical current by the photodiodes, and then to voltages by conditioning circuitry.

III. Measurements

An automated experimental setup is employed to reduce operator errors, see block diagram in Fig. 2. A 360° continuous motorized rotation stage NR360S/M (Thorlabs Inc.) [10] and a micro-stepping motor controller BSC201, are employed to adjust the rotation angles. Wing 2 of the optical sensor is fixed while wing 1 rotates under the guidance of the motorized stage. Overall system control is achieved using LabVIEW which involves implementing ActiveX interfacing technology for device control and performing data acquisition using a National Instrument card (NI USB-6211).

The conditioning circuitry converts the electrical current i, proportional to the illumination intensity (I), to voltages (V). Referring to (1) and (2), the voltages are obtained by the following equations.

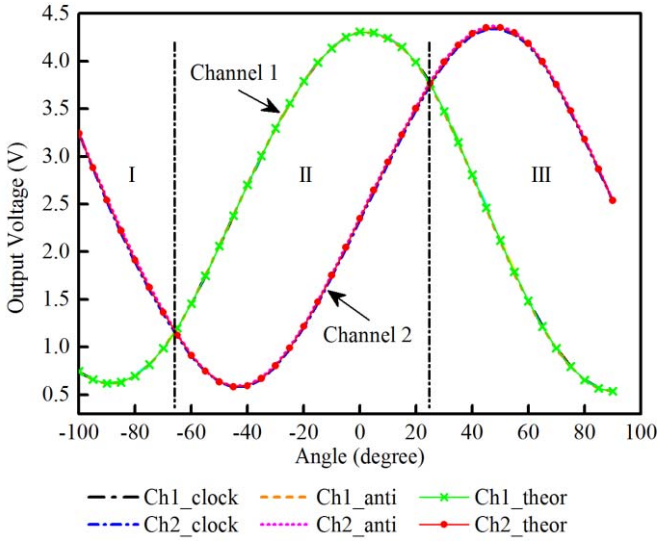

Fig. 4. The voltage-to-angle relationships of the optical sensor. Ch1_clock, Ch1_anti, and Ch1_theor represented the output readings from Channel 1 in clockwise and anticlockwise directions, and the theoretical values. Similarly, the Ch2_clock, Ch2_anti, and Ch2_theor were from Channel 2.

$$V_1 = k_1 \times i_1 + b_1 = m_1 \times I_1 + b_1 = m_1 \times I_0 \times \cos^2(\theta_1 - \theta_0) + b_1 = a_1 \times \cos^2(\delta_1) + b_1 \quad (3)$$

$$V_2 = k_2 \times i_2 + b_2 = m_2 \times I_2 + b_2 = m_2 \times I_0 \times \cos^2(\theta_2 - \theta_0) + b_2 = a_2 \times \cos^2(\delta_2) + b_2 \quad (4)$$

where the subscripts '1' and '2' represent the parameters for Channel 1 and Channel 2, respectively. δ_1 and δ_2 are the rotation angles relative to the polarization direction of P0. The parameters k_i, m_i and a_i (i=1, 2) denote the constants of proportionality, and b_i are constant voltages due to less than perfect blocking of light when the polarizers are set orthogonally.

In this paper, we define 0° to be the position when the sensor wings are in line with each other.

The measurements were carried out at room temperature with the motor rotating at 10°/s and data sampling at 100 Hz. The optical sensor was rotated from -100° to 90°, and then back to -100° in intervals of 5°. Each reading was composed of 500 samples. This process was repeated 5 times with an interval of 3 minutes between each cycle.

IV. Results and Discussions

A. Sensitivity and Hysteresis

Averaging the data over five cycles, leads to a voltage-to-angle relationship for both channels as plotted in Fig. 4. The theoretical values obtained from (3) and (4), are calculated and plotted as well.

The measured output voltages of both channels are consistent with the theoretical values. The maximum deviation from the theoretical voltages is 15% and occurs at the minimum outputs (approximately 60 mV). This is unsurprising since the signal is small and the sensitivity is a minimum. Additionally, both channels exhibited an identical response in both clockwise

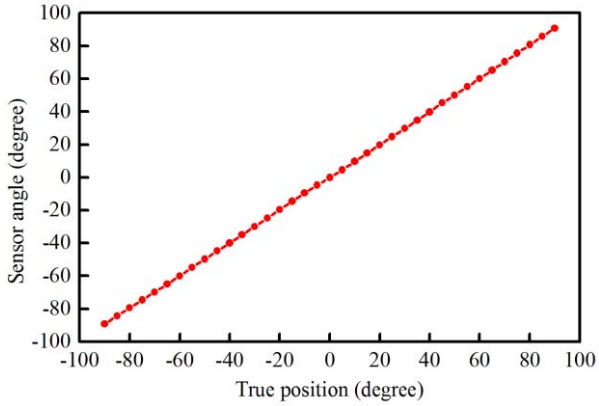

Fig. 5. The converted sensor angles versus the true position.

and anticlockwise directions with a hysteresis error less than 1.2%. The measurement span is limited to 90° for each channel, and the sensitivity is smallest at positions corresponding to maximum and minimum output readings.

B. *Angle Conversion*

To expand the measuring range and improve the sensor's sensitivity, we combine the information from two channels to obtain the angular position.

According to the amplitudes of both channels, the output voltages can be divided into three regions: I, II, and III (see Fig. 4). In region I and region III, the output of Channel 1 is smaller in amplitude compared to Channel 2. The opposite is true in region II. By comparing the amplitudes of each channel, we can select the channel operating in the linear region for that specific angle. By differentiating between the two channels in this way, we can effectively have a linear output spanning 180° combined with high sensitivity.

In order to avoid a high dependency on one channel, the weighted average method is used to calculate the angular position. For each channel, the rotation angles δ_1 and δ_2 is obtained by (3) and (4). Therefore, the final angle δ will be computed by (5).

$$\delta = w_1 \times \delta_1 + w_2 \times \delta_2 \tag{5}$$

where w_1 and w_2 denote the allocated different weights for Channel 1 and Channel 2, respectively.

There are various approaches to determine the weights. Considering the varying sensitivities in both channels, we allocate variable weights using (6) and (7) for δ_1 and δ_2. At each bending position (angle of articulation), the weights are determined by the closeness of the readings to the voltage at 45°.

$$w_1 = (1 - \frac{|V_1 - V_1(\delta_1 = 45)|}{|V_1 - V_1(\delta_1 = 45)| + |V_2 - V_2(\delta_2 = 45)|})^{3/2} \tag{6}$$

$$w_2 = 1 - w_1 \tag{7}$$

The converted sensor angle measured at each test position is shown in Fig. 5. The error bars for the output angle, too small to be seen in Fig. 5, are less than 0.1° and are determined from a standard uncertainty multiplied by a coverage factor of 3, which provides a confidence level of 99.7%. The data in Fig. 5 shows that the sensor has good full-scale accuracy (±0.5%) and excellent repeatability over the full 180° measurement range.

V. CONCLUSION

We have demonstrated our optical sensor with a wide measuring span (up to 180°), which is doubled compared to that achieved with our previous sensor. This enables the sensor to monitor the entire range of movement experienced by PIP, MCP, and other articulated joints in the human body. The accuracy and sensitivity has also been improved by adopting the weighted average approach to fuse output data.

The 3D printing technique is used to fabricate the sensor and a compact dimension with a diameter of 4.2mm and a width of 10 mm is achieved. This is sufficiently compact to be suitable for use on the hands of most adults. The optical sensor therefore has great potential for use as sensing elements in devices for hand motion tracking. In the future, we intend to focus on integrating this sensor into an instrumented glove system for real-time monitoring of hand motions.

REFERENCES

[1] L. Dipietro, A. M. Sabatini, and P. Dario, "A survey of glove-based systems and their applications," IEEE trans. Syst., Man, Cybern. C, Appl. Rev., vol. 38, no. 4, pp. 461-482, July 2008.

[2] D. J. Sturman and D. Zeltzer, "A survey of glove-based input," IEEE Comput. Graph. Appl., vol. 14, no. 1, pp. 30-39, January 1994.

[3] M. Amjadi, A. Pichitpajongkit, S. Lee, S. Ryu, and I. Park, "Highly stretchable and sensitive strain sensor based on silver nanowire-elastomer nanocomposite," ACS Nano., vol. 8, no. 5, pp. 5154-5163, April 2014.

[4] A. F. S. Silva, A. F. Gonc¸alves, P. M. Mendes, and J. H. Correia. "FBG sensing glove for monitoring hand posture," IEEE Sens. J., vol. 11, no. 10, pp. 2442-2448, October 2011.

[5] H. G. Kortier, J. Antonsson, H. M. Schepers, F. Gustafsson, and P. H. Veltink, "Hand Pose Estimation by Fusion of Inertial and Magnetic Sensing Aided by a Permanent Magnet," IEEE Trans. Neural Syst. Rehabil. Eng., vol. 23, pp. 796-806, September 2015.

[6] H. G. Kortier, V. I. Sluiter, D. Roetenberg, and P. H. Veltink, "Assessment of hand kinematics using inertial and magnetic sensors," J. Neuroeng. Rehabil., vol. 11, pp. 70, April 2014.

[7] L. Wang, T. Meydan, P. Williams, and T. Kutrowski, "A proposed optical-based sensor for assessment of hand movement," Sens. 2015 IEEE, Busan, pp. 1-4, November 2015.

[8] G. J. Wijntjes and C. T. Markos, "Non-contact optical polarization angle encoder," U.S. Patent 2005/0 002 032, January 2005.

[9] N. Albion, R. F. Asmar, R. W. Huggins, G. E. Miller, C. R. Porter, "Optical angle sensor using polarization techniques," U.S. Patent 5 424 535, June 1995.

[10] (2016) Thorlabs, Inc., [Online], Available: https://www.thorlabs.de/thorproduct.cfm?partnumber=NR360S/M.